short communications

The structure of a triple mutant of pI258 arsenate reductase from *Staphylococcus aureus* and its 5-thio-2-nitrobenzoic acid adduct

Joris Messens,[a]* **Inge Van Molle,**[a] **Peter Vanhaesebrouck,**[b] **Karolien Van Belle,**[a] **Khadija Wahni,**[a] **José C. Martins,**[b] **Lode Wyns**[a] **and Remy Loris**[a]

[a]Laboratorium voor Ultrastructuur, Vlaams Interuniversitair Instituut voor Biotechnologie (VIB), Vrije Universiteit Brussel, Pleinlaan 2, B-1050 Brussel, Belgium, and [b]NMR en Structuuranalyse eenheid, Universiteit Gent, Krijgslaan 281 S4, B-9000 Gent, Belgium

Correspondence e-mail:
joris.messens@vub.ac.be

Structural insights into formation of the complex between the ubiquitous thiol–disulfide oxidoreductase thioredoxin and its oxidized substrate are under-documented owing to its entropical instability. *In vitro*, it is possible *via* a reaction with 5,5'-dithiobis-(2-nitrobenzoic acid) to make a stable mixed-disulfide complex between thioredoxin from *Staphylococcus aureus* and one of its substrates, oxidized pI258 arsenate reductase (ArsC) from *S. aureus*. In the absence of the crystal structure of an ArsC–thioredoxin complex, the structures of two precursors of the complex, the ArsC triple mutant ArsC C10SC15AC82S and its 5-thio-2-nitrobenzoic acid (TNB) adduct, were determined. The ArsC triple mutant has a structure very similar to that of the reduced form of wild-type ArsC, with a folded redox helix and a buried catalytic Cys89. In the adduct form, the TNB molecule is buried in a hydrophobic pocket and the disulfide bridge between TNB and Cys89 is sterically inaccessible to thioredoxin. In order to form a mixed disulfide between ArsC and thioredoxin, a change in the orientation of the TNB–Cys89 disulfide in the structure is necessary.

1. Introduction

Arsenate reductase from *Staphylococcus aureus* (ArsC) is encoded by the plasmid pI258 *arsC* gene (Ji & Silver, 1992). ArsC plays a role in bacterial arsenate resistance and catalyses the reduction of arsenate to arsenite, which is subsequently exported from the cell. The structures of the oxidized and the reduced form of ArsC (Zegers *et al.*, 2001) and of the catalytically important intermediate forms have been solved (Messens, Martins, Van Belle *et al.*, 2002). ArsC has a PTPase I fold typical of low-molecular-weight tyrosine phosphatases (LMW PTPases; Fig. 1). The crystal structures of various mutants of ArsC in their reduced and oxidized forms, as well as a complex with arsenite, have been essential to unravel its reaction mechanism. The tetrahedral oxyanion arsenate binds in the active site (Messens, Martins, Brosens *et al.*, 2002), which has a typical P-loop structural fold (phosphate-binding loop; Fig. 1; Su *et al.*, 1994; Zhang *et al.*, 1994). For the reduction of arsenate, ArsC combines a phosphatase-like nucleophilic displacement reaction with a unique intra-molecular disulfide-bond cascade. Within this cascade, the formation of a disulfide bond triggers a 'conformational switch' (the formation of a Cys10–Cys82 disulfide) that transfers the oxidative equivalents to the surface of the protein while releasing the reduced substrate. Three essential redox-active cysteines (Cys10, Cys82 and Cys89; Messens *et al.*, 1999) are involved in the reduction of arsenate. After a single catalytic arsenate-reduction event, oxidized ArsC exposes a disulfide bridge between Cys82 and Cys89 on a looped-out redox helix (Fig. 1).

At the end of a single catalytic cycle, the reaction has to be completed and therefore oxidized ArsC has to be reduced by thioredoxin (Trx). In order to study the thiol–disulfide transfer interaction between thioredoxin and oxidized ArsC from *S. aureus* structurally, we prepared a mixed disulfide between ArsC and thioredoxin *via* a reaction with 5,5'-dithiobis-(2-nitrobenzoic acid) (DTNB). Previously, this *in vitro* approach has been exploited to visualize a thioredoxin–thioredoxin reductase complex (Lennon *et al.*, 2000; Wang *et al.*, 1996). Therefore, all cysteines inessential for the formation of the mixed disulfide partners (ArsC and thioredoxin) were replaced *via* mutagenesis. The ArsC C10SC15AC82S thus obtained was further modified by reaction with DTNB (φ-S-S-φ). As a result of the reaction, the remaining thiol of the ArsC triple mutant forms a mixed disulfide with 5-thio-2-nitro-benzoic acid (TNB) (ArsC-S-S-φ). In the next step, Trx C32S, which retains the essential catalytic Cys29, reacts with ArsC-S-S-φ. As such, a stable mixed-disulfide complex between the ArsC and thioredoxin was prepared (Messens *et al.*, 2004). Unfortunately, many attempts to crystallize this stable mixed-disulfide complex failed. In order to obtain

information on the structural state of ArsC before it engages in a thioredoxin–mixed disulfide complex, we determined the crystal structure of the triple mutant ArsC C10SC15AC82S in its free state and as a TNB adduct.

2. Experimental procedures

2.1. Site-directed mutagenesis, expression and purification

The ArsC triple mutant C10SC15AC82S was constructed, cloned into the pET14b vector to introduce an N-terminal His tag and expressed in *Escherichia coli* BL21(DE3). The ArsC C10SC15AC82S triple mutant was purified on Ni^{2+}–NTA Superflow (Qiagen, Valencia, CA, USA) in 20 mM Tris–HCl pH 7.9, 1 M NaCl, 0.1 mM EDTA, 2 mM 2-mercaptoethanol buffer solution and eluted with a 1 M imidazole linear gradient, followed by gel filtration on Superdex-75 HR (Amersham Biosciences, Uppsala, Sweden) in 20 mM Tris pH 8.0, 150 mM NaCl and 1 mM DTT (Messens *et al.*, 2004).

2.2. A thrombin digest to remove the N-terminal polyhistidine fused tag

To cleave the N-terminal His tag from ArsC C10SC15AC82S in 20 mM Tris pH 8.0, 150 mM NaCl and 1 mM DTT, thrombin (Sigma T7513) was added at 10 NIH units

per milligram of protein sample and incubated at 299 K. After 30 min, additional thrombin at 10 NIH units per milligram of protein was added and incubation continued for a further 30 min at 299 K. Thrombin was removed by adsorption onto a benzamidine Sepharose column (Amersham Biosciences, Uppsala, Sweden) equilibrated in 20 mM Tris–HCl pH 8.0, 100 mM NaCl. The flow-through of the column was loaded onto an Ni^{2+}–NTA Superflow (Qiagen, Valencia, CA, USA) column equilibrated with 20 mM Tris pH 7.9, 150 mM KCl, 0.1 mM EDTA buffer solution to remove the His-tag-containing fraction after the digest. The flowthrough fractions were pooled and reduced with 20 mM DTT. All buffer solutions were argon-flushed.

2.3. SDS–PAGE analysis and mass spectrometry

Samples were analysed on pre-casted 10% bis-tris NuPage SDS–PAGE with a SDS–MES running-buffer solution in an Xcell II Mini-Cell using the manufacturer's recommendations (Invitrogen, Carlsbad, CA, USA). Electrospray mass spectrometry was carried out with a Quattro II quadrupole mass spectrometer (Micromass, Manchester, UK) having an m/z range of 4000, as described previously (Messens *et al.*, 2000).

2.4. The reaction of ArsC C10SC15AC82S with TNB

Purified ArsC triple mutant without histidine tag was treated with DTT by incubation with 20 mM fresh DTT at room temperature for 30 min to assure full thiol reduction. The excess of DTT was removed on a Superdex-75 HR (10/30) column equilibrated in 20 mM Tris–HCl pH 8.0, 150 mM KCl, 50 mM K_2SO_4 and 0.1 mM EDTA. The fractions containing ArsC were pooled and an excess of DTNB (10 mM) (Sigma, St Louis, MI, USA) was added. The completion of the reaction was monitored at 412 nm. The volume of the reaction mixture was reduced on a 5 kDa cutoff concentrator (Vivascience, Lincoln, UK) and then applied for a second time to the gel-filtration column in order to remove excess DTNB and released TNB^-. The fraction containing the mixed disulfide ArsC C10SC15AC82S–TNB adduct after the gel-filtration column was concentrated on a Vivaspin 5 kDa cutoff concentrator.

2.5. Crystallization of ArsC C10SC15AC82S and ArsC C10SC15AC82S–TNB

ArsC C10SC15AC82S after cleavage of the polyhistidine tag (MW = 15 029.8 Da; $\varepsilon_{0.1\%}^{280}$ = 1.685) was concentrated on a Vivaspin 5 kDa cutoff concentrator to an OD_{280} of 28.6 and dialyzed against 20 mM Tris pH 8.0, 100 mM KCl buffer solution. ArsC C10SC15AC82S was crystallized at 293 K using the hanging-drop vapour-diffusion method with 50 mM Tris pH 8.0, 100 mM $NaClO_4$, 42.5%(w/v) PEG 4000 as reservoir solution (1 ml). The ArsC drop (3 µl) was mixed with an equal volume of precipitant solution and 1 µl 1%(w/v) agarose dissolved in 50 mM Tris pH 8.0. The agarose was added to improve crystal quality.

The ArsC C10SC15AC82S–TNB adduct (Messens *et al.*, 2004) without histidine tag (OD_{280} = 26.6) in 20 mM Tris pH 8.0, 100 mM KCl buffer solution was crystallized with the same precipitant solution as described above. The ArsC drop (1 µl) was mixed with an equal volume of precipitant solution.

2.6. Data collection and structure determination

Data from ligand-free ArsC C10SC15AC82S were collected using an ADSC Quantum Q4R CCD detector at station ID14-2 of the ESRF synchrotron, Grenoble, France and data from the mixed disulfide complex ArsC C10SC15AC82S–TNB were collected on a MAR CCD
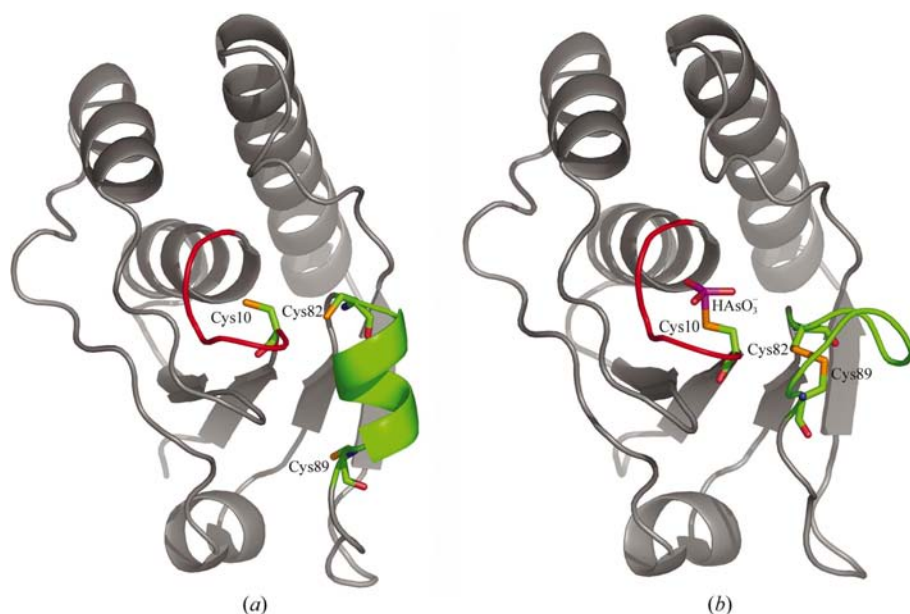

Figure 1
(*a*) The structure of wild-type ArsC in the reduced state (PDB code 1ljl). The short redox helix bearing Cys82 and Cys89 (green) is structured. (*b*) The structure of ArsC C15A in the oxidized state (PDB code 1lju). The short redox helix is looped-out (green). In this structure, arsenite is bound in the active site P-loop. In both structures, the redox-active cysteines (in stick representation) and the P-loop active site (red) are shown. The figures were prepared using the program *PyMol* 0.9 (DeLano Scientific).

detector at station BW7A of the DESY synchrotron, Hamburg, Germany. Diffraction images were processed using the programs *DENZO*, *XDisplayF* and *SCALEPACK* from the *HKL* package (Otwinowski & Minor, 1997) and the *CCP*4 program *TRUNCATE* (Collaborative Computational Project, Number 4, 1994). The structures were determined by molecular replacement using *AMoRe* (Navaza, 1994) with reduced ArsC C10SC15A (PDB code 1jf8) as a model. Refinement was performed using the maximum-likelihood target function based on structure factors in the *CNS* program (Brünger *et al.*, 1998). The TNB molecule was built manually using the program *TURBO* (Roussel & Cambillau, 1989). *CNS* topology and parameter files for TNB were constructed using the Dundee ProDrg2 server (van Aalten *et al.*, 1996) available at http://davapc1.bioch.dundee. ac.uk/programs/prodrg/prodrg.html. Bulk-solvent and anisotropic *B*-factor corrections were used throughout the refinement.

3. Results and discussion

While His-tagging of proteins results in a fast and easy purification method, it is also known to have an influence on their solubility and as such may compromise the crystallization conditions (Hammarstrom *et al.*, 2002; Rosenow *et al.*, 2002). Therefore, we removed the His tag of the ArsC triple mutant by thrombin digestion. Thrombin digestion followed by a benzamidine Sepharose and immobilized metal-affinity chromatography resulted in almost complete recovery of ArsC C10SC15AC82S. We obtained a reasonably high final purification yield of approximately 21 mg per litre
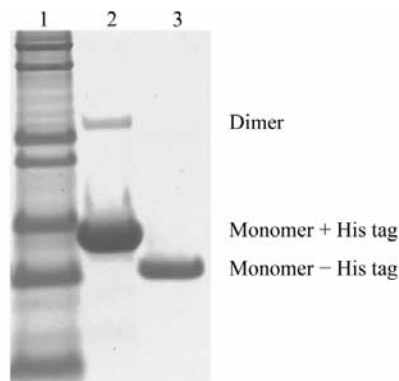

Figure 2
Analysis of the ArsC C10SC15AC82S on SDS-PAGE. Lane 1, M12 protein markers (Invitrogen) of 66.3, 55.4, 36.5, 31, 21.5, 14.4 and 6 kDa; lane 2, purified ArsC C10SC15AC82S containing the polyhistidine tag; lane 3, purified ArsC C10SC15AC82S without the His tag after thrombin digest.

Table 1
Data-collection and refinement statistics.

Values in parentheses are for the last shell.

	ArsC C10SC15AC82S	ArsC C10SC15AC82S–TNB$^-$
PBD code	1rxi	1rxe
Resolution limits (Å)	23.9–1.5 (1.55–1.5)	25–1.7 (1.75–1.7)
Space group	$P2_1$	$P2_12_12_1$
Unit cell-parameters (Å, °)	$a = 32.0$, $b = 34.1$, $c = 63.4$, $\beta = 97.3$	$a = 33.1$, $b = 34.4$, $c = 102.3$
Wavelength (Å)	0.998	0.998
Measured reflections	102023	37303
Unique reflections	21553	11893
Completeness (%)	98.1 (95.8)	88.1 (80.6)
R_{merge} (%)	6.4 (27.7)	7.1 (35.8)
$I/\sigma(I)$	12.96 (3.05)	9.92 (2.89)
Refinement statistics		
R_{work}/R_{free}† (%)	20.9/23.1	19.5/21.2
R.m.s. deviation, bonds (Å)	0.0064	0.0058
R.m.s. deviation, angles (°)	1.37	1.44
No. waters	199	125
Ligands	K$^+$, Cl$^-$, ClO$_4^-$	K$^+$, ClO$_4^-$, MNB‡ (TNB)
Ramachandran profile		
Core region (%)	94.8	93.9
Additionally allowed (%)	5.2	6.1
Disallowed (%)	0.0	0.0

† $R_{work} = \sum |F_{obs} - F_{calc}|/\sum |F_{obs}|$ using 95% of the total reflections for the refinement. R_{free} was calculated as R_{work} using 5% of the total reflections which were not used in the refinement. ‡ 5-Mercapto-2-nitrobenzoic acid.

of culture. The purity was checked on SDS–PAGE (Fig. 2). The ArsC–TNB adduct was prepared as described in §2.4. The triple mutant ArsC C10SC15AC82S and its TNB adduct have the expected molecular weights of 15 030 and 16 780 Da, respectively. The triple mutant ArsC C10SC15AC82S as well as its TNB adduct crystallize under the same conditions as previously described for oxidized SeMet ArsC C10SC15A (Zegers *et al.*, 2001) and their structures were solved by molecular replacement. The data-collection and refinement statistics are shown in Table 1.

The structure of ArsC C10SC15AC82S closely resembles that of the reduced form of wild-type ArsC, with an r.m.s.d. of 0.58 Å for 130 C$^\alpha$ atoms (Fig. 3). The largest structural variation is observed in the Lys109–Phe114 segment, a region that is not close to the mutation sites or the active site. This variation is a consequence of differences in crystal contacts and does not arise from the mutation or from the absence of a bound perchlorate in the active site of the wild-type structure. Indeed, the reduced state of the ArsC double mutant C10SC15A, which also features a tetrahedral oxyanion in its active site but has an isomorphous structure to the wild-type protein, shows the same differences from the triple mutant as does the wild type.

One of the available structures of an oxidized form of ArsC comes from the ArsC C10SC15A double mutant (Zegers *et al.*, 2001), in which a disulfide bridge is formed between Cys82 and Cys89. A large conformational change is seen in the Cys82–Lys97

stretch of the oxidized protein compared with the reduced form (Fig. 1). Consequently, the r.m.s.d. for all the C$^\alpha$ atoms between oxidized and reduced ArsC C10SC15A is 1.28 Å. This compares well with a value of 1.36 Å for the superposition of oxidized ArsC C10SC15A on the triple mutant.

The TNB adduct of ArsC C10SC15AC82S is isomorphous to the reduced forms of ArsC C10SC15A and the wild-type protein. As the ArsC adduct is a precursor for the production of a stable covalent ArsC–Trx complex *in vitro*, it was expected that the TNB molecule would be solvent-exposed and its disulfide linkage with Cys89 accessible to thioredoxin. However, in the crystal structure the TNB molecule, which shows up very clearly in the electron-density maps (Fig. 4a), is buried in a hydrophobic pocket formed by Ile9, Ile39, Ile67, Leu72, Val78 and Pro90 (Fig. 4b). This results in a small local conformational rearrangement in the loop around Cys89 (Asn87–Leu92), which moves 2.5 Å to accommodate the TNB molecule (Fig. 3a). TNB binding does not interfere with the binding of arsenate in the P-loop active site, which is also the binding site of other tetrahedral oxyanions (sulfate, perchlorate; Messens, Martins, Brosens *et al.*, 2002). The polar carboxylate and nitro groups of TNB point towards the solvent and do not form any hydrogen bonds with the protein. The temperature factors of the TNB molecule are rather high (about 40 Å^2) relative to those of the surrounding protein atoms (15–20 Å^2). The electron density is nevertheless clear and together with the

absence of any suggestion for alternative conformations, it is most likely that the TNB molecule is bound with full occupancy. The higher temperature factors are thus most likely to be a consequence of a non-specific binding mode in a pocket that is not optimized to harbour this non-natural ligand. Although the TNB molecule does not make any direct contacts with a symmetry-related ArsC molecule, a water bridge is found between its nitro group and the side chain of Lys127 from a symmetry mate. However, as the physiologically relevant conformation of the mixed disulfide is not known, it cannot be excluded that the currently observed conformation is selected by the crystal packing.

The structural changes seen upon formation of the adduct are reminiscent of those seen in small-to-large mutations to induce

strain in the hydrophobic core of T4 lysozyme (Liu *et al.*, 2000). Overall, the structure of the adduct form still closely resembles the reduced form of ArsC, with an r.m.s.d. of 0.84 Å for all C^α atoms. In all structures of the reduced form of ArsC (wild-type, C10SC15A and C10SC15AC82S) the free thiol group of Cys89 is located in the same hydrophobic pocket. Partial exposure of Cys89 occurs upon the transition towards the oxidized structure, which is the form recognized by thioredoxin. The mixed disulfide observed in our crystal structure is certainly not a physiologically relevant structure. It is most likely that its conformation is driven by the hydrophobic interactions between the benzyl ring of TNB and the hydrophobic pocket of ArsC (Fig. 4). The Val77–Lys98 region is known to be flexible and the orientation of Cys89 in the

structure is here determined by the presence of TNB.

Thus, in the conformation observed in our crystal structure of the ArsC triple mutant adduct, a nucleophilic attack of Cys29 from Trx C32S towards the TNB disulfide bridge is avoided. Nevertheless, it was possible to construct a stable mixed-disulfide complex using the TNB adduct (Messens *et al.*, 2004), suggesting conformational fluctuations of this region in solution. Previously, we observed by NMR that the formation of a disulfide bridge between Cys10 and Cys82 induces conformational fluctuations of the complete redox-helix region (residues of the segment Val77–Lys98) on the microsecond to millisecond time scale (Messens, Martins, Van Belle *et al.*, 2002). Furthermore, in the crystal structure of the oxidized form of ArsC C89L (PDB code 1lk0) featuring the Cys10–Cys82 disulfide, the two molecules in the asymmetric unit have different conformations for the stretch of residues 82–97. One molecule has a partially folded redox helix with a conformation similar to that of reduced ArsC (Fig. 1*a*) and the other a partially unfolded redox helix which resembles the oxidized form of ArsC (Fig. 1*b*). Although the redox helix of the ArsC triple mutant (PDB code 1rxi) is structured, it might have an increased intrinsic flexibility, which is supported by the much faster H/D exchange rate of amide moieties in the redox helix compared with other α-helical segments (unpublished results). Knowing that the redox-helix region of ArsC has a tendency to undergo a conformational change, it might well be that different structural orientations of this region are present in solution, but only the structure with a hidden TNB molecule crystallized (Fig. 3).

4. Conclusions

The ArsC C10SC15AC82S triple mutant has the same structure as wild-type ArsC with a folded redox helix. To our surprise, the TNB molecule in the adduct form of the triple mutant was hidden in a hydrophobic pocket and was not present on the looped-out redox helix on the surface of ArsC. The disulfide bridge between Cys89 and TNB was found to be sterically inaccessible to nucleophilic attack of Cys29 from thioredoxin. Nevertheless, a stable mixed-disulfide complex was prepared between ArsC C10SC15AC82S and Trx C32S *via* a reaction with DTNB (Messens *et al.*, 2004). A different structural orientation of the TNB–Cys89 disulfide on the flexible redox helix is necessary in order to form this complex. We believe that local
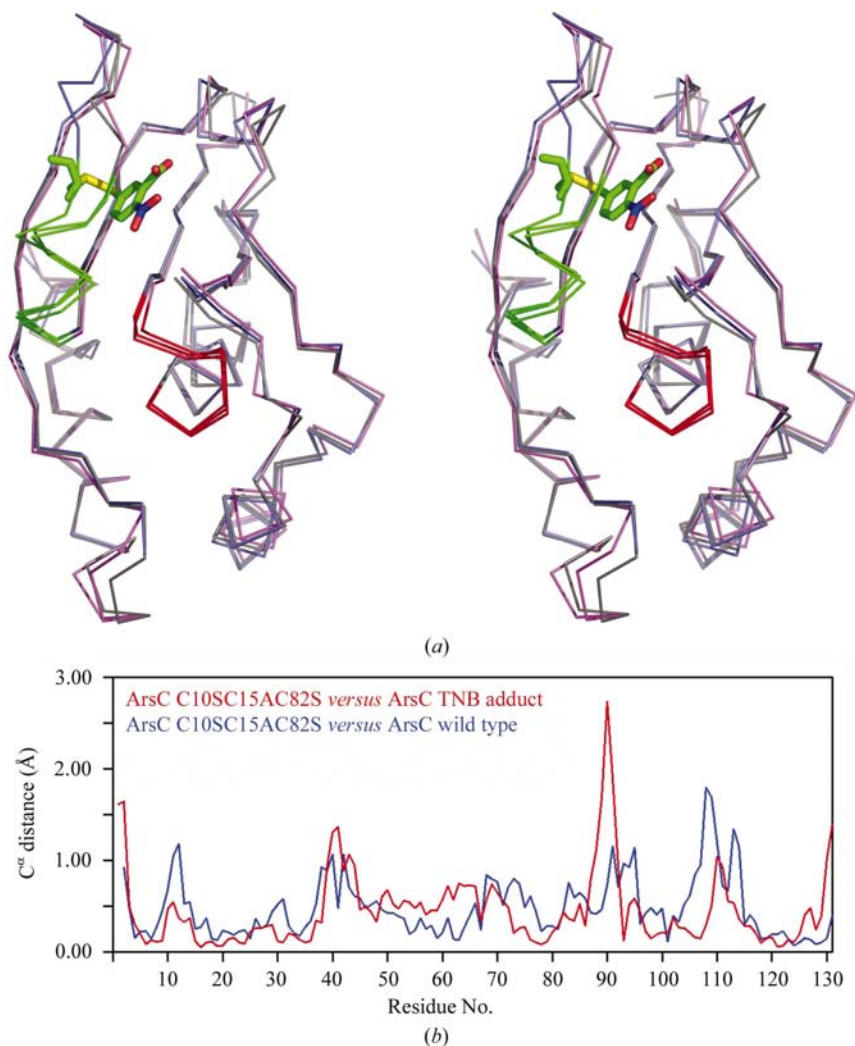

Figure 3
(*a*) A stereoview of the ribbon diagram of the overall structure of ArsC C10SC15AC82S (grey) and its TNB adduct form (slate) fitted on top of the structure of reduced wild-type ArsC (violet). The redox helix (green) and the P-loop (red) are shown. TNB and Cys89 are shown in stick representation. The figure was prepared using *PyMol* 0.9 (DeLano Scientific). (*b*) Plot of the C^α distances between C10SC15AC82S and the wild-type reduced ArsC (blue) and the TNB adduct (red) after optimal superposition of all equivalent C^α pairs.
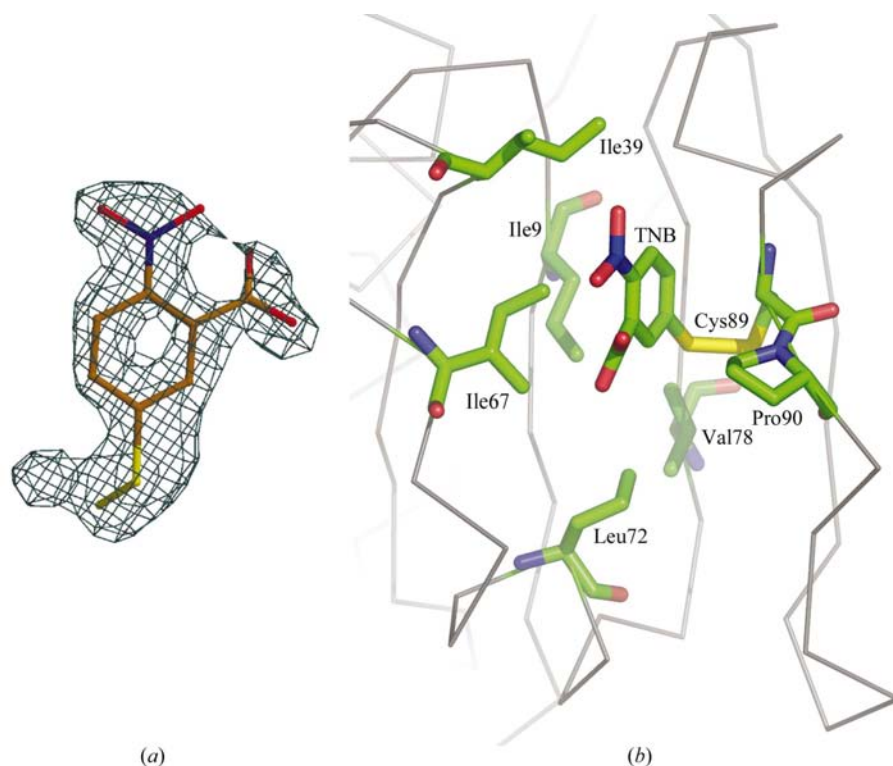
short communications

Figure 4
(a) $F_o - F_c$ omit electron-density map of 5-thio-2-nitrobenzoate (TNB) bound to Cys89 in the structure of C10SC15AC82S (PDB code 1rxe) at 1.7 Å. The map is contoured at 3.0σ. Figure prepared using the program *MOLSCRIPT* (Kraulis, 1991). (b) The TNB molecule as observed in its structural hydrophobic environment. The figure was prepared using *PyMol* 0.9 (DeLano Scientific).

structural heterogeneity arising from a number of small redox-helix variations might also be responsible for crystallization failure in the mixed-disulfide complex between ArsC and thioredoxin.

References

Aalten, D. M. F. van, Bywater, R., Findlay, J. B. C., Hendlich, M., Hooft, R. W. W. & Vriend, G. (1996). *J. Comput. Aided Mol. Des.* **10**, 255–262.
Brünger, A. T., Adams, P. D., Clore, G. M., DeLano, W. L., Gros, P., Grosse-Kunstleve, R. W., Jiang, J.-S., Kuszewski, J., Nilges, M., Pannu, N. S., Read, R. J., Rice, L. M., Simonson, T. & Warren, G. L. (1998). *Acta Cryst.* D**54**, 905–921.
Collaborative Computational Project, Number 4 (1994). *Acta Cryst.* D**50**, 760–763.
Hammarstrom, M., Hellgren, N., van Den Berg, S., Berglund, H. & Hard, T. (2002). *Protein Sci.* **11**, 313–321.
Ji, G. & Silver, S. (1992). *J. Bacteriol.* **174**, 3684–3694.
Kraulis, P. J. (1991). *J. Appl. Cryst.* **24**, 946–950.
Lennon, B. W., Williams, C. H. & Ludwig, M. L. (2000). *Science*, **289**, 1190–1194.
Liu, R., Baase, W. A. & Matthews, B. W. (2000). *J. Mol. Biol.* **295**, 127–145.
Messens, J., Hayburn, G., Brosens, E., Laus, G. & Wyns, L. (2000). *J. Chromatogr. B*, **737**, 167–178.
Messens, J., Hayburn, G., Desmyter, A., Laus, G. & Wyns, L. (1999). *Biochemistry*, **38**, 16857–16865.
Messens, J., Martins, J. C., Brosens, E., Van Belle, K., Jacobs, D. M., Willem, R. & Wyns, L. (2002). *J. Biol. Inorg. Chem.* **7**, 146–156.
Messens, J., Martins, J. C., Van Belle, K., Brosens, E., Desmyter, A., De Gieter, M., Wieruszeski, J. M., Willem, R., Wyns, L. & Zegers, I. (2002). *Proc. Natl Acad. Sci. USA*, **99**, 8506–8511.
Messens, J., Van Molle, I., Vanhaesebrouck, P., Limbourg, M., Van Belle, K., Wahni, K., Martins, J. C., Loris, R. & Wyns, L. (2004). In the press.
Navaza, J. (1994). *Acta Cryst.* A**50**, 157–163.
Otwinowski, Z. & Minor, W. (1997). *Methods Enzymol.* **276**, 307–326.
Rosenow, M. A., Magee, C. L., Williams, J. C. & Allen, J. P. (2002). *Acta Cryst.* D**58**, 2076–2081.
Roussel, A. & Cambillau, C. (1989). *TURBO-FRODO. Silicon Graphics Geometry Partners Directory*, pp. 71–78. Mountain View, CA, USA: Silicon Graphics.
Su, X. D., Taddei, N., Stefani, M., Ramponi, G. & Nordlund, P. (1994). *Nature (London)*, **370**, 575–578.
Wang, P. F., Veine, D. M., Ahn, S. H. & Williams, C. H. J. (1996). *Biochemistry*, **35**, 4812–4819.
Zegers, I., Martins, J. C., Willem, R., Wyns, L. & Messens, J. (2001). *Nature Struct. Biol.* **8**, 843–847.
Zhang, Z. Y., Wang, Y., Wu, L., Fauman, E. B., Stuckey, J. A., Schubert, H. L., Saper, M. A. & Dixon, J. E. (1994). *Biochemistry*, **33**, 15266–15270.